NUCLEAR SCIENCE AND TECHNIQUES **26**, 010102 (2015)

# The macromolecular crystallography beamline of SSRF*

WANG Qi-Sheng (汪启胜),[1,2] YU Feng (郁峰),[1] HUANG Sheng (黄胜),[1] SUN Bo (孙波),[1]
ZHANG Kun-Hao (张坤浩),[1] LIU Ke (刘科),[1] WANG Zhi-Jun (王志军),[1] XU Chun-yan (徐春艳),[1]
WANG Si-Sheng (王思胜),[1] YANG Li-Feng (杨利峰),[1] PAN Qiang-Yan (潘强岩),[1] LI Liang (李良),[1]
ZHOU Huan (周欢),[1] CUI Yin (崔莹),[1] XU Qin (徐琴),[1] Thomas Earnest,[1] and HE Jian-Hua (何建华)[1,†]

[1]*Shanghai Institute of Applied Physics, Chinese Academy of Sciences, Shanghai 201800, China*
[2]*University of Chinese Academy of Sciences, Beijing 100049, China*

(Received September 24, 2014; accepted in revised form November 17, 2014; published online February 2, 2015)

The macromolecular crystallography beamline BL17U1 at the Shanghai Synchrotron Radiation Facility (SSRF) is the first dedicated macromolecular crystallography (MX) beamline at a third-generation synchrotron in China. It utilizes an in-vacuum undulator as a source and is energy-tunable from 5 to 18 keV. The beamline was commissioned and opened for users in April 2009. The experimental station was upgraded in 2011 with an advanced detector, a high precision goniometer and an automatic sample exchanger for high efficient and high-throughput data collection of protein crystals. The current set-up allows for remote operation of sample mounting, centering and data collection of pre-frozen crystals. In recent two years, the number of PDB depositions from this beamline exceeds 330 each year. In this paper, we describe the complete BL17U1 beamline with upgraded end station and how it is managed for user community.

Keywords: Macromolecular crystallography, Beamline automation

DOI: 10.13538/j.1001-8042/nst.26.010102



## I. INTRODUCTION

The Shanghai Synchrotron Radiation Facility (SSRF) is a national facility dedicated to scientific research requiring synchrotron light [1]. The phase-I beamlines serve the user community with a wide range of applications in physics, chemistry and life sciences. Among them, BL17U1 is a dedicated macromolecular crystallography (MX) beamline. It is the first third-generation MX beamline in China and makes structure biologists in China more easily accessible to synchrotron beam time for MX. It was designed to meet various demands on crystal structural determination of large unit cell and small crystals as well. The high flux with small beam divergence and reasonably small beam size facilitate structural determination of large complexes up to 1000 Å unit cell and small crystals down to a few tens of micron size. It is tunable in the range of 5–18 keV, with the flux around $4 \times 10^{12}$ photons/s at 1 Å. Performance of the beamline was examined and verified by committee of international experts. It was available for users in April 2009. In initial stage, the end-station was equipped with a MarDTB and Mar225 CCD (Charge-Coupled Device) detector due to limited budget. In the upgrade project of the end station approved by Chinese Academy of Sciences (CAS), the end-station was equipped with an ADSC 315 CCD detector and a high precision goniometer from Crystal Logical. To improve the operation efficiency and achieve full automation of the experiment, a robotic sample exchanger from Rigaku was installed and integrated to the control system with friendly interface. In this paper, we describe the upgraded end-station of the beamline, the user's activity and the productivity, and their fruitful results.

## II. BEAMLINE OVERVIEW

SSRF, a third-generation light source with a 3.5 GeV storage ring of 432 m circumference and 3.9 nm rad emittance, has been in operation since 2009. Many improvements in performance have been made to meet experimental demands of the users [2]. Currently top-up mode with 240 mA ring current is the routine operational mode for users.

A home-made in-vacuum undulator with 80 periods and a period length of 2.5 cm [3] serves as the source. Its parameters are optimized to cover the required energy range (5–18 keV) with easy tuning allowing typical SAD (Single-wavelength Anomalous Dispersion) or MAD (Multi-wavelength anomalous dispersion) experiments and with brilliant beam of ~ $10^{19}$ photons/[(mm$^2$mrad$^2$s(0.1 %BW)]. The source size is 380 μm × 25 μm (FWHM, H×V) and flux in the central cone (80 × 20 μrad$^2$@12 keV) is $3.0 \times 10^{14}$ ph/[s(0.1 %BW)]. A water-cooled aperture defines the size of the emitted photon beam. The beamline has an optical set-up well suited for the finely collimated undulator beam. The layout is shown in the Fig. 1.

To build an easy-use and reliable crystallography beamline, the optical design is the pursuit of high stability and high flux. The beamline optical components include a double plane crystal monochromator (DCM) and a toroidal mirror that focuses the beam both vertically and horizontally. The DCM is a central unit of the optical system manufactured by ACCEL Instruments GmbH. The double crystal monochromator is located at 27.5 m from the source. Due to the extremely high heat-load power density on the first crystal of the DCM, it is cooled by liquid nitrogen (LN), the Si(111) flat

* Supported by the Shanghai Synchrotron Radiation Facility Phase-I project and the Upgrading project of Chinese Academy of Sciences (2010)
† Corresponding author, hejianhua@sinap.ac.cn

TABLE 1. Specifications of beamline BL17U1

| | |
|---|---|
| Source Type | Undulator, 25 mm × 80 periods, 6–12 mm gap |
| Monochromator | Cryo-cooled double flat crystal Si(111) |
| X-ray energy range (keV) | 5–18 |
| Wavelength range (Å) | 0.69–2.48 |
| Flux at sample (at 12.4 keV 240 mA)[a] (phs/s) | $3.8 \times 10^{12}$ |
| Focused beam size (FWHM) (μm) | 67 × 23 (H×V) |
| Typical beam divergence (mrad) | ~ 0.3 × 0.1 |
| Goniometer | Single-axis |
| Cryo capability (K) | 100 |
| Sample mounting | Manually/Rigaku ACTOR robot |
| Detector model | CCD, Q315r |
| 2Theta capability | None |

[a] Measured by using a calibrated ion chamber close to sample position with the 7th harmonic of U25.

first crystal, sized as 150 mm($l$) × 30 mm($w$) × 30 mm($h$), is mounted on an LN-cooled copper heat exchanger. The second flat crystal is sized as 170 mm($l$)×30 mm($w$)×30 mm($h$). The DCM deflects the beam upwards with a fixed 25 mm offset in the energy range. A separate water chiller is installed to help the internal thermally stability, which is vital to stability of the beamline. Temperature of the thermal stabilization system is monitored by PT100 sensors placed at different points in the DCM chamber.

The focusing mirror,which is manufactured by Thales SESO, with a toroidal surface obtained by bending a cylinder, deflects the beam horizontally in 3.5 mrad grazing angle. It focuses the beam horizontally by dynamically tunable meridional curvature, and vertically by a fixed sagittal curvature. In this optical geometry, the beam exiting from the toroidal mirror is parallel to the ground, which facilitates the beamline alignment and experimental setup. The dimension of the mirror is 1000 mm($l$) × 70 mm($w$) × 50 mm($h$), with 50 nm rhodium coating on the silicon substrate. The mirror is mounted on the bender manufactured by Toyama Co., Ltd.

The beam position monitoring system for monitoring and diagnosing the beam includes a fluorescence screen, a wire-scan beam probe and a quadrant beam position monitor (QBPM) [4]. The fluorescence screen that can be inserted into the beam to inspect of the white and monochromatic beams, and the wire that can be scanned to probe the beam profile, are mainly used in the commissioning stage, while the foil QBPM can stay in the beam for data recording of the beam stability. There are two beryllium windows located after the DCM and mirror, respectively, to protect the components in ultra-high vacuum. The beamline is tunable over the range of 0.69–2.48 Å, though it is usually operated in the 0.8–1.8 Å range. The flux of focused beam at 1 Å is ~ $3.8 \times 10^{12}$ phs/s ( and Table 1).

## III. EXPERIMENTAL ENVIRONMENT

In the experimental hutch, the monochromatic beam passes through a rotary attenuator consisting of aluminum foils of various thicknesses, so as to provide an attenuated X-ray beam based on the users' choice. The first ionization chamber probes the intensity, directly linked to the piezoelectric-based optimizing program on the second crystal of DCM to keep the maximum intensity and a constant beam position. The overview of the end station, the environment around the sample, and one tab of the graphical user interface are shown in the Fig. 3.

### A. End station hardware

A micro-goniometer (Crystal Logical LA, USA) is installed on a separate stand from the detector support table, so as not to affect the sample-beam alignment when changing the detector distance. The air-bearing spindle has a vertical motion for an accurate beam-sample alignment to the X-ray beam. The beam-conditioning components located in the goniometer arm include a fast shutter, which is synchronized with the rotary axis, two slits and one micro ionization chamber. The slits combined with the micron ion chamber are used for auto optimization when the energy is changed or after long term operation. An active beam stop is installed after the sample to block the beam and monitor the intensity [5]. The sample is visualized from a top view and an on-axis view. For optical position relied on the on-axis camera is a dual lens system with two fixed magnifications: the low magnification for finding the loop easily, while the high magnification for precise crystal positioning. The digital image is displayed on a browser window and integrated into the BluIce control software. Centering of the crystal is performed via a click-to-center procedure from the software interface.

The Mar 225 CCD was replaced by ADSC Q315r detector (Area Detector System Corporation, Poway, USA) in Oct 2010. The sample-detector distance is changeable from 85 to 1000 mm, corresponding to a maximum detectable resolution of 0.98 Å at 1 Å wavelength, for the circle inscribed in the ADSC detector square face. A resolution predictor is automatically updated when the detector position changes.

The Oxford Cryosystem 700 (Oxford, UK) keeps the sample at 100 K in standard operation. A Hitachi vortex Si-drift detector can be moved pneumatically close to the sample for MAD scans and X-ray excitation experiments to determine the optimal energy for data collection. In order to meet the need for data collection on extremely small crystals, a micro-collimator which offers 20, 10 and 5 μm apertures is under development.

Samples can be mounted either manually or by the ACTOR sample changer (Rigaku, USA) that has a capacity of 80 pre-cooled samples in its storage Dewar. Uni-pucks with 18 mm standard pins are recommended. Routine calibration and maintenance ensure the reliability and an increasing number of crystals have been screened easily since the installation of ACTOR, as shown in Fig. 4.

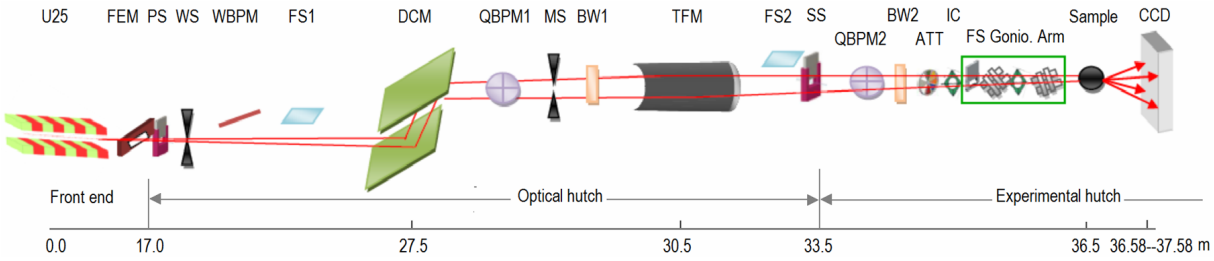


Fig. 1. (Color online) Beamline layout with relative distances (not to scale) from the light source. U25, in-vacuum undulator; FEM, front-end beam defining mask; PS, photon shutter; WS, white beam slit; WBPM, a scanable cross wires white beam BPM; FS1, white beam fluorescence screen; DCM, double crystal monochromator; QBPM1, monitor for monochromator beam after DCM; MS, mono beam slit; BW, beryllium window; TFM, toroidal focusing mirror; FS2, mono beam fluorescence screen; SS, safety shutter; QBPM2 monitor for mono beam before the exit Be window; ATT, attenuation; IC, ionization chamber; Gonio ARM (shown in green box) includes a fast shutter, two slits and an ionization chamber. annually.

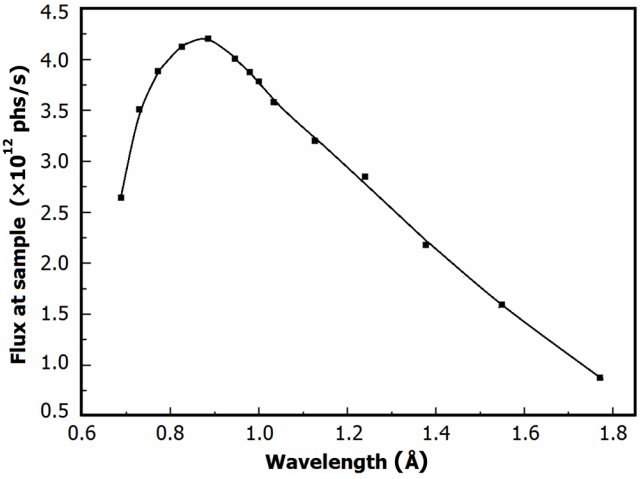


Fig. 2. Flux over the wavelengths range available to the users. Currently full focus beam is used only. The development on minibeam to collimator is underway.

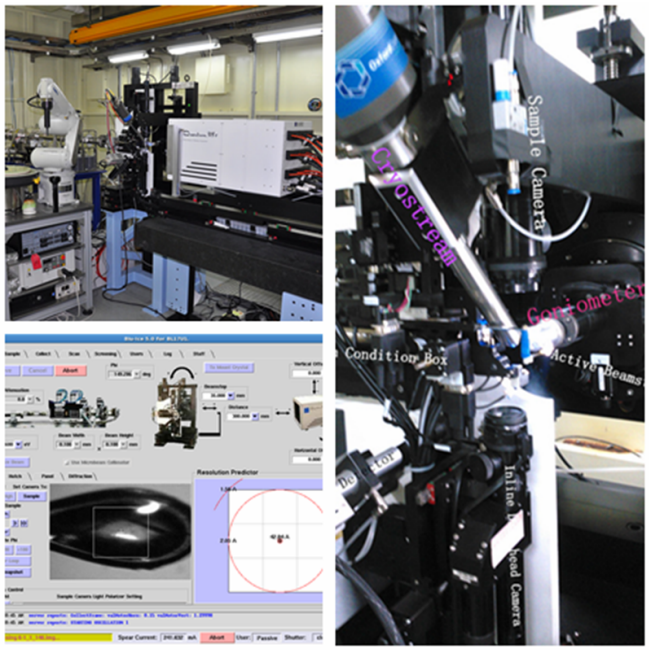


Fig. 3. (Color online) The BL17U1 end station (upper-left) and the tabbed GUI (lower-left). The environment around the sample (right) includes the goniometer, cameras, cryosystem, beam condition box and fluorescence detector.

### B. Software

The EPICS (Experimental Physics and Industrial Control System) Input Output Controllers (IOCs) are running on VME crates for the motor control and signal readout. Linux-based IOCs are also running for other module devices, such as the Galil motor controller and axis network devices. Our strategy is to put as much as possible under EPICS to minimize code, with good flexibility. The beamline components controlled by EPICS are implemented by the control group [6] of the Phase I beamlines. The operator interface of EPICS is just suitable for engineering level, but the BL17U1 users request integrated control and data acquisition system including all the components and functions of beamline and end station with intuitive tabbed graphical user interface GUI (Graphical User Interface). The Blu-Ice/DCS (Distributed Control System), developed at SSRL [7] and implemented on many beamlines, is extensively utilized by the international user community. Based on the DCSS (distributed control system server) protocol, the program EPICS gateway translates messages between the EPICS CA (Channel Access) protocol and the DCS protocol. A few new DHS (distributed hardware server) are developed for specific devices, such as the sample exchanger and the fluorescence detector. The sequencing and scientific functions are implemented by the script engine, including the automatic beamline optimization, the energy synchronization and the undulator gap during energy scan, the click-to-center, and so on. More details on the control and data acquisition system can be found elsewhere [8]. The automatic crystal-centering, especially for positioning tiny crystals, is required by the users, and this function is being integrated. The functional system with intuitive GUI ensures that the beamline is easy-to-use and reliable.

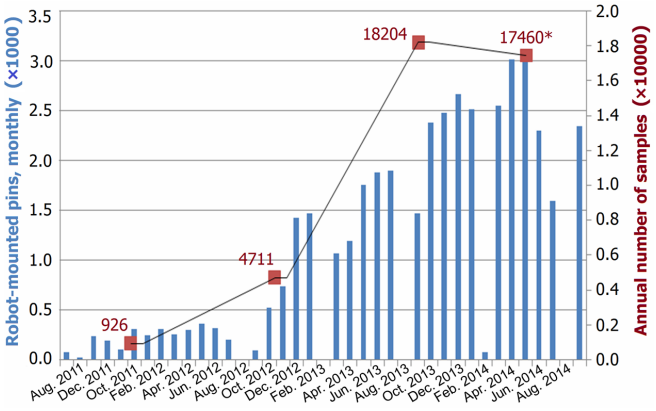


Fig. 4. (Color online) The number of pins mounted by the ACTOR sample changer. The blue bars are robot-mounted pins in months for the users' programs, while the red marks are annual number of samples. The robot was introduced to users in August 2011. As of September 2014, 41301 samples were mounted by the robot for sample screening and data collection.

## IV. ANCILLARY FACILITY

An auxiliary laboratory nearby the beamline has been built for macromolecular crystallography users. The lab provides conditions for the users to prepare protein crystal samples on site. It is equipped with a number of equipment and instruments, including incubator shakers, centrifuges, AKTA (GE Healthcare Life Sciences) purifier, ultraviolet spectrophotometer, nanoparticle size analyzer, nanoliter high-throughput liquid handing system, stereomicroscopes, etc. The users can carry out experiments of protein expression, protein purification and crystal growth in the lab. Two thermostatic chambers at 277 K and 291 K respectively can be used by the users to purify proteins, grow crystals and store crystal samples. Also, tools for flash freezing crystals and soaking heavy atoms are provided for the users to prepare crystals. They can harvest the diffraction data immediately after sample preparation in the lab so as to reduce effect of transportation and other environmental change. The uni-puck is also provided to the novice users.

The beamline control and data processing is performed from the control area adjacent to the experimental hutch. All computers are managed by Open LDAP (Open Lightweight Directory Access Protocol) for account authorization. The data storage is 16TB over 1GB/s connection with all the computers of the beamline. Data processing and analysis software commonly used by protein crystallographers are available, including *HKL2000* [9], *iMosflm* [10], *XDS* [11], *CCP4i* [12], *PHENIX* [13], *SHELX* [14] and other related programs. Since beam time is extremely oversubscribed, the users are encouraged to process the dataset as soon as possible and backup their data to their disks after their beam time slot. Due to the limited storage, the diffraction images are saved on the server for one month currently.

## V. FACILITY ACCESS

Users must complete typical safety training and pass the related examination to carry on experiment on BL17U1 beamline. Its beam time for general users can be obtained through four mechanisms running in parallel. These will mostly vary in the leading time before being scheduled, ranging from half a year to a week. The first one is the regular user proposal access program. SSRF receives this kind of proposal twice every year, with the deadline on 30$^{th}$ March and 30$^{th}$ September, respectively. The proposals are reviewed and scored by the external panel based on their scientific merit and technical feasibility of the research plan. The proposals are required to be submitted online at the website of http://ssrf.sinap.ac.cn/proposals. The second one is the fast access mode that can be submitted at any time by contacting the beamline staff during the year giving access on a very short time basis for one particular experimental visit, but this mode accounts for less than 10% of the total user beam time. Since 2010, the third mode, so called as awarded beamtime, has been allocated for the users who did outstanding work on the beamline, based on the SCI impact factor of the papers. Beamtime for this kind access is about 20% of the total user beamtime now, because of explosive growth in publication. Since 2012, the fourth one, long-term proposals for two year period, with the deadline of 30$^{th}$ June, have been received by the beamline and allotted through peer-review. The amount of this kind is about 15% of the total user beamtime. Typically an allocated beamtime slot is three quarters of an eight-hour shift for utilizing the beamline efficiently. In the past five years, the average ratio 22% of the required beamtime from users is satisfied, as shown in Fig. 5.

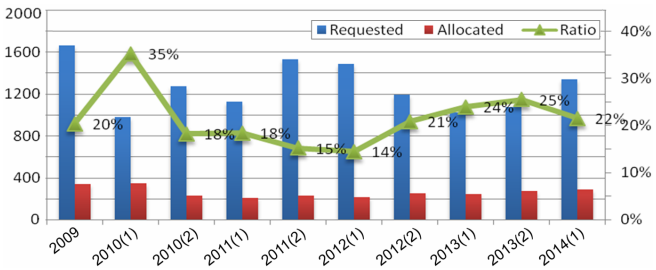


Fig. 5. (Color online) The statistics on the requested and the allocated beam time, demonstrating that the beamline is seriously oversubscribed.

Operation of the beamtime stimulated research enthusiasm from pharmaceutical companies, too. The industrial user needs are valued by the facility, thus 10% of the user beamtime is reserved to these users. Fourteen pharmaceutical companies have carried out their projects already on the beamline.

Since the end of 2012, the remote access has been opened to users after we made a series tests [15]. The users who have previous experience with the beamline and robot are welcomed to use the remote access for the data collection. The authorized users may access the beamline control software GUI remotely to carrying out their experiment via a security NoMachine NX session. Users can fully run the beamline

from their home laboratory just as if they were on site. The remote access will be routine in very near future.

## VI. PRODUCTIVITY

Commissioned in April 2009, BL17U1 enters into its 6th year of operation. Now, BL17U1 accommodates annually over 180 groups, including users of academic institutions and pharmaceutical companies. It has been productive both in terms of publications and Protein Data Bank (PDB) depositions over the past five years. The number of structures keeps increasing year by year. According to statistics by the Biosync (http://biosync.sbkb.org), BL17U1 ranked No. 1 in 2012 in the number of structures by data-collected from a single beamline. Considering the delay of the deposited structure to PDB, the number of 2013 still in increase will likely exceed the number of 2012.

The number of articles published is in explosive growth. Experiments on BL17U1 have yielded several important results in structural biology [16–19]. Up to September 2014, 33 papers were published in Cell, Science and Nature. Fig. 6 shows the statistical data up to 10th October, 2014.

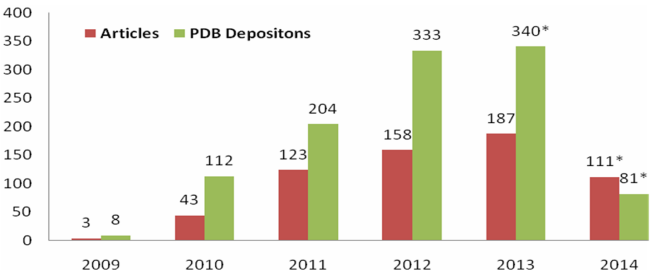


Fig. 6. (Color online) The structures publicly deposited to PDB since the beamline opened to users. The PDB data are taken from the Biosync website (http://biosync.sbkb.org). The data of 2013 and 2014 is still incomplete due to the lag to public.

### A. MAD/SAD: ECF transporter

The energy-coupling factor (ECF) transporters constitute a novel family of conserved membrane transporters in prokaryotes that have a similar domain organization to the ATP-binding cassette transporters. Yigong Shi group solved the 3.5 Å structure of an ECF transporter [20] that is believed to be specific for hydroxymethyl pyrimidine. The structures enable them to propose a plausible working model for the transport cycle of the ECF transporters. There are no mammalian homologues for the S-protein components of ECF transporters, and the molecules have a notably high substrate-binding affinity, suggesting potential targets for much-needed new antibiotics. This is one of the projects performed on BL17U1 that took advantage of MAD and SAD methods for structure determination.

### B. High resolution: LGN/NuMA and LGN/mInsc complexes

Asymmetric cell division requires the establishment of cortical cell polarity and the orientation of the mitotic spindle along the axis of cell polarity. Par3/Par6/aPKC protein complexes are involved in the establishment and maintenance of cell polarity. NuMA/LGN/Gαi protein complexes are involved in the regulation of spindle orientation. Adaptor protein mInscuteable (mInsc) connect Par3/Par6/aPKC and NuMA/LGN/Gαi protein complexes. Therefore, these protein complexes play an important role in asymmetric cell division. Previous studies have confirmed that in invertebrates, with the adapter protein mInscuteable (mInsc) connected Par3/Par6/aPKC complex and NuMA/LGN/Gαi complexes playing a key role in asymmetric cell division process. However, molecular mechanisms of interaction of LGN-NuMA and LGN-mInsc complex are not yet clear. The Minjie Zhang group solved the structures of the LGN/mInsc and LGN/NuMA complexes. Their results suggest that the Par3/mInsc/LGN and NuMA/LGN/Gαi complexes may play sequential and partially overlapping roles in asymmetric cell division. The molecular basis for the binding of LGN to NuMA and mInsc is well understood based on the 1.10 Å high-resolution structures of the LGN/NuMA and LGN/mInsc complexes [21].

### C. Large cell constants:EV71

Human enterovirus 71 (EV71) is the leading causative agent for severe hand-foot-and-mouth diseases (HFMD) in infants and young children. Uncoating is essential in EV71 life cycle, which is characterized by conformational changes in the capsid to facilitate RNA release into host cell. Rong Chen group have solved the EV71 virus structure in uncoating status which crystallized in the space group I23 with the large cell dimensions of a=b=c= 591.38 Å [22]. Structure comparison of the full virion and uncoating intermediate enable them to map the conformational changes associated with uncoating and provide a more detailed picture to understand the early steps of EV71 uncoating.

## VII. DISCUSSION AND PERSPECTIVE

As the first dedicated MX beamline in a third-generation synchrotron radiation facility in China, BL17U1 is well designed and operated. To gain experience, we made a verification process at the beginning to check the performance. The beamline performance is routinely checked by collecting datasets from lysozyme crystals and resolving the structure by S-SAD (Sulfur-SAD) at 1.5 Å. This kind routine self-inspection can assure that everything of the beamline is functioning well, especially avoiding the misalignment the rotator axis and the beam. The beamline operation attracted the nationwide users and several groups from neighboring countries. Although we tried our best to offer as much as

possible beam time for users, the beamline is still oversubscribed. Our flexible access mode, the streamline data collection software with intuitive interface, and the hardware, allows the beamline to be competitive and as productive as other beamlines of more modern synchrotrons in the world. The efficient beam time scheduling, sometimes within a few hours of a request, accelerate the process of users' research projects. The 24-h on site support is available during users experiment. Our group, consisting of members from many disciplines, contributes to the high quality support to users.

In addition, the hardware and software are improved continuously to meet requirements from more challenging projects. For example, a smaller beam size will be achieved by implementing compound refractive lens to facilitate data collection of micro-crystals. The new functions, such as rastering for centering crystal from opaque background and data processing pipeline, are being developed and evaluated towards greater scientific productivity.

## ACKNOWLEDGEMENTS

The authors gratefully acknowledge those colleagues who used to work for the beamline, in particular Tang Lin, Chen Mingzhi, Sun Lihua and Zhou Xiang, and the support groups of the SSRF, particularly the technicians and engineers. Without their participation, the development, construction, and operational success of beamline BL17U1 would have been impossible.



[1] Jiang M H, Yang X, Xu H J, *et al*. Shanghai Synchrotron Radiation Facility. Chin Sci Bull, 2009, **54**: 4171–4181. DOI: 10.1007/s11434-009-0689-y

[2] Zhao Z T, Yin L X, Leng Y B, *et al*. Performance optimization and upgrade of the ssrf storage ring. Proceedings of IPAC13, Shanghai, China, 2013, 178–180.

[3] Zhang W, Zhou Q G, Wang H F. The performance optimization for two in-vacuum undulators in SSRF. Sientia Sinica Phys Mechanica Astron, 2011, **41**: 2–5. (in Chinese) DOI: 10.1360/132010-680

[4] Alkire R W, Rosenbaum G, Evans G. Design of a vacuum-compatible high-precision monochromatic beam-position monitor for use with synchrotron radiation from 5 to 25 keV. J Synchrotron Radiat, 2000, **7**: 61–68. DOI: 10.1107/S090904959901568X

[5] Pan Q Y, Wang Q S, Wang Z J, *et al*. An active beam-stop for accurate measurement of high intensity X-ray beams. Nucl Instrum Meth A, 2014, **735**: 584–586. DOI: 10.1016/j.nima.2013.10.011

[6] Liu P, Zhou Y N, Mi Q R, *et al*. EPICS-based data acquisition system on beamlines at SSRF. Nucl Tech, 2010, **33**: 415–419. (in Chinese)

[7] McPhillips T M, McPhillips S E, Chiu H J, *et al*. Blu-Ice and the Distributed Control System: software for data acquisition and instrument control at macromolecular crystallography beamlines. J Synchrotron Radiat, 2002, **9**: 401–406. DOI: 10.1107/S0909049502015170

[8] Wang Q S, Huang S, Sun B, *et al*. Control and data acquisition system for the macromolecular crystallography beamlines of SSRF. Nucl Tech, 2012, **35**: 5–11. (in Chinese)

[9] Otwinowski Z and Minor W. Processing of X-ray diffraction data collected in oscillation mode. Methods Enzymol. 1997, **276**: 307–326. DOI: 10.1016/S0076-6879(97)76066-X

[10] Battey T G G, Kongtogiannis L, Johoson O, *et al*. IMOSFLM: a new graphical interface for diffraction-image processing with MOSFLM. Acta Crystallogr D, 2011, **67**: 271–281. DOI: 10.1107/S0907444910048675

[11] Kabsch W. Automatic processing of rotation diffraction data from crystals of initially unknown symmetry and cell constants. J Appl Crystallogr, 1993, **26**: 795–800. DOI: 10.1107/S0021889893005588

[12] Bailey S. The CCP4 suite: programs for protein crystallography. Acta Crystallogr D, 1994, **50**: 760–763. DOI: 10.1107/S0907444994003112

[13] Adams P D, Grosse-Kunstleve R W, Hung L W, *et al*. PHENIX: building new software for automated crystallographic structure determination. Acta Crystallogr D, 2002, **58**: 1948–1954. DOI: 10.1107/S0907444902016657

[14] Sheldrick G M. A short history of SHELX. Acta Crystallogr A, 2008, **64**: 112–122. DOI: 10.1107/S0108767307043930

[15] Wang Q S, Sun B, Huang S, *et al*. Remote access of the beamline BL17U at Shanghai Synchrotron Radiation Facility. Acta Crystallogr A, 2014, **70**: C796.

[16] Deng D, Yan C, Pan X, *et al*. Structural basis for sequence-specific recognition of DNA by TAL effectors. Science, 2012, **335**: 720–723. DOI: 10.1126/science.1215670

[17] Shi Y, Zhang W, Wang F, *et al*. Structures and receptor binding of hemagglutinins from human-infecting H7N9 influenza viruses. Science, 2013, **342**: 243–247. DOI: 10.1126/science.1242917

[18] Wu D, Hu Q, Yan Z, *et al*. Structural basis of ultraviolet-B perception by UVR8. Nature, 2012, **484**: 214–219. DOI: 10.1038/nature10931

[19] Hu L L, Li Z, Cheng J, *et al*. Crystal structure of TET2-DNA complex: Insight into TET-mediated 5mC oxidation. Cell, 2013, **155**: 1545–1555. DOI: 10.1016/j.cell.2013.11.020

[20] Wang T, Fu G, Pan X, *et al*. Structure of a bacterial energy-coupling factor transporter. Nature, 2013, **497**: 272–276. DOI: 10.1038/nature12045

[21] Zhu J, Wen W, Zheng Z, *et al*. LGN/mInsc and LGN/NuMA complex structures suggest distinct functions in asymmetric cell division for the Par3/LGN and Gαi/LGN/NuMA pathways. Mol Cell, 2011, **43**: 418–431. DOI: 10.1016/j.molcel.2011.07.011

[22] Lyu K, Ding J, Han J F, *et al*. Human enterovirus 71 uncoating captured at atomic resolution. J Virol, 2014, **88**: 3114–3126. DOI: 10.1128/JVI.03029-13